PERGAMON

Vision Research 42 (2002) 1683–1693

Vision Research

www.elsevier.com/locate/visres

Age-related changes in refractive index distribution and power of the human lens as measured by magnetic resonance micro-imaging in vitro

B.A. Moffat [a], D.A. Atchison [b], J.M. Pope [a,*]

[a] *Centre for Medical, Health and Environmental Physics, Queensland University of Technology, G.P.O. Box 2434, Brisbane 4001, Australia*
[b] *Centre for Eye Research, Queensland University of Technology, G.P.O. Box 2434, Brisbane 4001, Australia*

Received 13 August 2001; received in revised form 22 January 2002

Abstract

We report a new technique for non-invasively mapping the refractive index distribution through the eye lens using magnetic resonance micro-imaging. The technique is applied to map the refractive index distribution throughout the sagittal plane of 18 human eye lenses ranging in age from 14 to 82 years in vitro. The results are compared with standard models for the human eye lens. They confirm that the refractive index distribution, when plotted as a function of normalised lens radius, is a function of lens age and differs both between the equatorial and axial directions and between the anterior and posterior halves of the optical axis. The refractive index of the lens nucleus exhibits a significant reduction with age amounting to $3.4 \pm 0.6 \times 10^{-4}$ years^{-1}. The contribution of the gradient index (GRIN) to the lens power decreases by 0.286 ± 0.067 D/year, accounting almost entirely for the estimated overall change in lens power with age for these lenses, which were probably in their most accommodated state. The results provide experimental verification of hypothesised changes in the GRIN that have previously been invoked as contributing to presbyopia and support the hypothesis that changes in the GRIN are sufficient to offset effects of increasing curvature of human lenses with age in their unaccommodated state.

Keywords: Eye lens; Refractive index; Gradient index; Magnetic resonance imaging

1. Introduction

It has been known for about 100 years (Gullstrand, 1909) that the refractive index of the human eye lens is inhomogeneous, exhibiting a 'gradient index'. In the Gullstrand number one eye the lens was considered to have a nucleus with a uniform refractive index of 1.406, surrounded by a cortex with a refractive index of 1.386. Most other models of the eye have simplified the index distribution even further by assuming a lens with a uniform 'equivalent refractive index' (e.g. Emsley, 1952). However the human lens is now known to exhibit a continuous gradient of refractive index (GRIN) (Nakao, Fujimoto, Nagata, & Koiti, 1968; Nakao & Ono, 1969; Pierscionek & Chan, 1989). The refractive index distribution in the human lens is believed to contribute significantly to the total lens power (Smith & Pierscionek, 1998; Smith, Pierscionek, & Atchison, 1991), giving the lens an equivalent refractive index which is higher than that of either the nucleus or the cortex and which typically falls in the range between 1.44 and 1.41 depending on age (Dubbelman & Van der Heijde, 2001a,b).

Modelling the effects of a GRIN on the optical properties of the lens can be performed with great precision (Atchison & Smith, 1995; Garner & Smith, 1997; Hemenger, Garner, & Ooi, 1995; Pierscionek, Chan, Ennis, Smith, & Augusteyn, 1988; Smith, Atchison, & Pierscionek, 1992; Smith et al., 1991), but obtaining experimental data on the lens GRIN is not trivial. Pierscionek and Chan (1989) developed a non-destructive ray tracing method for mathematically deriving the refractive index distribution in the equatorial plane, that relied on the circular cross-section of the lens in this plane. However the refractive index distribution in the equatorial plane is of limited relevance to the optics of the lens because it does not contain the lens optical axis. It is the refractive index in the sagittal plane that

* Corresponding author. Tel.: +61-7-3864-2325; fax: +61-7-3864-1804.
E-mail address: j.pope@qut.edu.au (J.M. Pope).

0042-6989/02/$ - see front matter
PII: S0042-6989(02)00078-0

determines the lens optical properties, but in this plane the human lens is not circular in cross-section but approximately biconvex. This added complexity means that ray tracing results in this plane cannot be directly used to derive the refractive index distribution without making assumptions concerning the shape of the GRIN (Pierscionek & Chan, 1989).

Pierscionek et al. (1988) transposed the refractive index distribution in the equatorial plane to the sagittal plane of the lens, based on an assumption that the lens grows uniformly in the radial direction by the layering of new fibre cells over the existing lens. To do this it must be further assumed that the three dimensional isoindical contours of the lens are concentric and follow the shape of the lens. Such assumptions have been shown to work quite well for the bovine lens, but for human lenses the method could not accurately predict the ray paths in the sagittal plane (Pierscionek et al., 1988).

Pierscionek (1997) also used a reflectometric optical sensor to measure the refractive index both along the optical axis and in the equatorial plane of several human lenses. She found differences in the shape of the refractive index distribution along these axes, which were inconsistent with the assumption of three dimensional concentric isoindical contours in the human lens. Although these measurements showed that it is invalid to assume the existence of concentric isoindical contours in the sagittal plane through the centre of the lens, the detailed shape of the refractive index contours could not be measured because of the invasive nature of this one dimensional technique. Despite this, transposition of the equatorial distribution to the sagittal plane has been widely used to model the human lens (Garner & Smith, 1997; Hemenger et al., 1995; Smith et al., 1992). Using these modelling techniques (Smith et al., 1992; Smith & Pierscionek, 1998) it has been shown that changes to the shape of the GRIN could plausibly lead to a loss of refractive power and a decrease in accommodative ability with age. Currently there are no findings that have provided experimental verification of such changes to the lens GRIN shape. Consequently, two-dimensional experimental measurements of the refractive index distribution in the sagittal plane are needed to obtain a better understanding of the influence of the GRIN on human lens optics, to provide experimental evidence of changes to the lens GRIN with age and to improve human lens models.

In this study we used magnetic resonance imaging (MRI) to measure the refractive index distribution in the sagittal plane of the human lens non-invasively. The results of these in vitro measurements on lenses of various ages have implications for a better understanding of changes that occur in the aging lens, notably the onset of presbyopia and the 'lens paradox'—the observation that, while the curvature of the lens surface (in the unaccommodated state), increases with age (Brown, 1974), this occurs without the eye at the same time tending to myopia (Koretz & Handelman, 1986).

2. Theory

Since the link between the optical and magnetic resonance properties of the human eye lens is not obvious, we first present some theory that establishes a theoretical relationship between them for protein solutions. The refractive index of protein solutions has been known for some time to be linearly related to the protein concentration, by the Gladstone–Dale formula (Barer & Joseph, 1954):

$$n = n_0 + \frac{\mathrm{d}n}{\mathrm{d}c}c \tag{1}$$

where c is the concentration of protein in units of mass per unit volume, n is the refractive index of the solution and n_0 is the refractive index of the solvent. The dry weight of the lens is mainly comprised of lens-specific proteins, in the form of α, β and γ crystallins. Consequently the refractive index of the human lens is a linear function of the local protein concentration (Pierscionek, Smith, & Augusteyn, 1987). The refractive index at any point in the three dimensional lens can therefore be expressed as

$$n(x,y,z) = n_0 + \frac{\mathrm{d}n}{\mathrm{d}c}c(x,y,z) \tag{2}$$

where $n(x,y,z)$ and $c(x,y,z)$ are now the local refractive index and crystallin concentration, respectively.

In nuclear magnetic resonance (NMR) and MRI, the magnetisation of the sample is perturbed by application of radiofrequency pulses. Its return to equilibrium is characterised by two relaxation times, the longitudinal or 'spin–lattice' relaxation time T_1, that characterises the return to equilibrium of the component of magnetisation parallel to the applied static magnetic field, and the transverse or 'spin–spin' relaxation time T_2 that is the time constant for decay of components of magnetisation perpendicular to the static field (e.g. Callaghan, 1991). For a wide range of protein solutions, it has also been shown empirically that the transverse relaxation rate for water protons ($R_2 = 1/T_2$) is linearly dependent on protein concentration (Hills, Takacs, & Belton, 1989), at least within specific concentration ranges

$$R_2 = A + \frac{\mathrm{d}R_2}{\mathrm{d}c}c \tag{3}$$

where A is an empirical constant. For protein solutions, $\mathrm{d}R_2/\mathrm{d}c$ is always positive, so that the relaxation mechanism becomes more efficient as the concentration of protein increases. This increase in relaxation efficiency is due to chemical exchange between the water protons and the NH moieties of the proteins (Hills et al., 1989). Since such chemical exchange relies on the proteins

being soluble, the parameter c in Eq. (3) is strictly the concentration of soluble proteins. Eq. (3) can be substituted into Eq. (1) to give a theoretical relationship between protein concentration and transverse relaxation rate:

$$n = B + \frac{\mathrm{d}n}{\mathrm{d}R_2} R_2 \tag{4}$$

where

$$B = n_0 - \frac{\mathrm{d}n}{\mathrm{d}R_2} A \tag{5}$$

Using standard MRI techniques (Callaghan, 1991; Pelc, 1993), two-dimensional maps of the spatial distribution of R_2 over a selected slice or plane through the lens can be readily acquired. The R_2 value for each particular picture element or pixel within the image is thus related to the local refractive index such that:

$$n(x,y,z) = B + \frac{\mathrm{d}n}{\mathrm{d}R_2} R_2(x,y,z) \tag{6}$$

where $R_2(x,y,z)$ is the R_2 value corresponding to the pixel of interest. If the R_2 map is taken through the central sagittal plane ($x = 0$) then $n(0,y,z)$ is a map of the refractive index distribution in the sagittal plane.

The paraxial power of the lens with such a refractive index distribution can be estimated from equations derived by Smith et al. (1992) and Smith and Pierscionek (1998). Firstly the total lens power can be expressed as

$$F = F_1 + F_{\mathrm{GRIN}} + F_2 - \frac{d_1 F_1 F_{\mathrm{GRIN}}}{n_{\mathrm{e}}} - \frac{d_2 F_{\mathrm{GRIN}} F_2}{n_{\mathrm{e}}} - \frac{(d_1 + d_2) F_1 F_2}{n_{\mathrm{e}}} + \frac{d_1 d_2 F_1 F_2 F_{\mathrm{GRIN}}}{n_{\mathrm{e}}^2} \tag{7}$$

where F_1 and F_2 are the contributions to lens power of the lens surfaces, given by

$$F_1 = \frac{(n_{\mathrm{e}} - 1.336)}{R_1} \quad \text{and} \quad F_2 = \frac{(1.336 - n_{\mathrm{e}})}{R_2} \tag{8}$$

and where R_1 and R_2 are the anterior and posterior radii of curvature, n_{e} is the lens surface refractive index, d_1 and d_2 are the distances from the lens surfaces on the optical axis to the first and second principal planes of the GRIN, respectively and F_{GRIN} is the contribution to lens power of the GRIN.

Smith and Pierscionek (1998) used a bi-elliptical model for the human lens developed by Smith et al. (1991). In this model the refractive index distribution was given by a sixth order polynomial of the form:

$$n = n_0 + n_1 r^2 + n_2 r^4 + n_3 r^6 \tag{9}$$

where n_0 is the lens central refractive index, n_1, n_2, and n_3 are coefficients that describe the shape of the refractive index distribution, and r is the normalised radius from the centre of the lens ($r = 0$) to its surface, where $r = 1$ in any direction. For such a lens model Atchison and Smith (1995) showed that the GRIN contribution to the paraxial power of the lens, (F_{GRIN}), could be expressed as

$$F_{\mathrm{GRIN}} \approx -2\left(n_1 + \frac{2}{3} n_2 + \frac{3}{5} n_3\right) \frac{t}{b^2} \tag{10}$$

where t is the thickness and b is the semi-diameter of the lens. It will be shown that all the parameters in Eqs. (7), (8) and (10) can be obtained from the $n(0,y,z)$ maps such that the paraxial power of the lens can be estimated.

3. Methods

Human lenses were obtained from the Queensland and NSW Eye Banks. All lenses were stored at 34.5 °C in artificial aqueous humour (AAH) after removal from the eye. The AAH was made in sterile conditions using Auto-Pow minimum essential medium with Earl's salts (MEME: ICN Biochemicals, Costa Mesa, CA), with the addition of HEPES (10 mM), glutamine (2 mM), penicillin (1000 $\mu g\,l^{-1}$), streptomycin (1 $mg\,l^{-1}$), amphotericin (10 $mg\,l^{-1}$) and adjusted to a pH of 7.4. Twenty porcine lenses (less than 12 h post-mortem) and eight human lenses (less than 2 days post-mortem) were used to make lens homogenates with varying concentrations of lens crystallins spanning the range of values found in the intact lens. Lenses were stripped of their outer capsule and placed in an empty sample container. A glass rod and stainless steel spatula were then used to homogenise them by hand. The porcine lens homogenate with the highest refractive index was made from porcine lens nuclei (~5 in number) while the other porcine homogenates were made from a mixture of cortical and nuclear tissue, diluted with AAH as appropriate to cover the required refractive index range. The human lens homogenates were made from eight lenses donated by individuals ranging in age from 50–68 years. In all cases the lenses used contained no visible sign of cataract. Again the homogenates corresponding to the lower values of refractive index were derived from a mixture of material from lens cortex and nucleus, while higher values of refractive index were derived primarily from nuclear material and in one case this was further concentrated by evaporation at 23 °C. The refractive index of each solution was measured using an Abbe refractometer with a white light source.

Measurements of transverse relaxation time T_2 were made on a Bruker MSL200 NMR spectroscopy/microimaging system, using a standard Carr–Purcell/Meiboom–Gill (CPMG) pulse sequence (Carr & Purcell, 1954; Meiboom & Gill, 1958), with the homogenate samples in sealed 5 mm diameter NMR tubes. The refractive index measurements were repeated immediately after the NMR data had been acquired to ensure that

any dehydration during the NMR measurements would have minimal impact on the results.

In order to quantitatively map T_2 (or R_2) over a thin slice through the lens we required an MRI pulse sequence capable of measuring T_2 with sufficient accuracy that the results could be compared directly with the spectroscopic (non-imaging) measurements on the homogenates. This was achieved by employing a standard 'spin echo' imaging sequence with CPMG pre-weighting of the equilibrium magnetisation (Moffat, 2001; Pelc, 1993). In each pixel of the image the signal can be expressed as

$$S = S_0' \mathrm{e}^{-2\tau n R_2} \tag{11}$$

where n is the number of 180° R.F. pulses in the CPMG pre-weighting, 2τ is the time between the 180° pulses and S_0' incorporates signal weighting due to choice of parameters associated with the imaging segment of the pulse sequence. A series of T_2 weighted images of $CuSO_4$ solutions at room temperature was acquired using this pulse sequence. The results were in good agreement with values obtained by spectroscopic (non-imaging) methods.

For acquisition of intact human eye lens R_2 maps in vitro, the lenses were contained in standard 10 mm NMR tubes surrounded by AAH. Initial 'scout' images were acquired in different planes to ensure the final image plane included the optical (symmetry) axis of the lens. The images for construction of the R_2 maps were then acquired using $n = 1$ to 10 π pulses in the CPMG pre-weighting (where $\tau = 2.1$ m s), a field of view (FoV) = 28 mm, slice thickness = 1 mm, and 128×128 pixel resolution. The relatively large FoV was chosen in order to improve pixel signal-to-noise ratio (S/N) without resorting to unduly long imaging times. Each pixel was fitted to Eq. (11) using a modified Levenberg–Marquart algorithm in MATLAB® to produce the R_2 maps.

4. Results

Examples of signal decays due to T_2 relaxation in human lens homogenates of different protein concentration, measured spectroscopically are shown in Fig. 1. All were found to be well fitted by mono-exponential decay functions. Fig. 1 also shows that the decay rates (R_2) are significantly different for the different homogenates. A plot of refractive index (n) as a function of R_2 (Fig. 2) exhibits a strong and significant linear correlation ($r^2 = 0.98$, $p < 0.0001$) between n and R_2 for human lens homogenates. The linear equation relating n to R_2 was found to be

$$n = 1.355 + 1.184 R_2(\mathrm{m\,s^{-1}}) \tag{12}$$

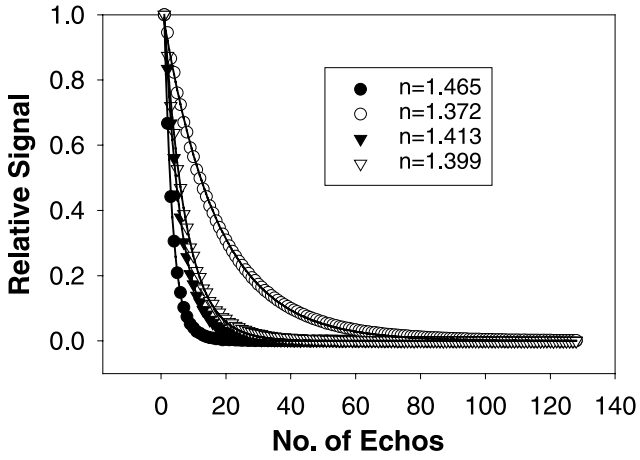

Fig. 1. T_2 decays of human lens homogenates with different protein concentrations and refractive indices acquired at 34.5 °C. The data are well fitted by a mono-exponential decay in all cases (—).

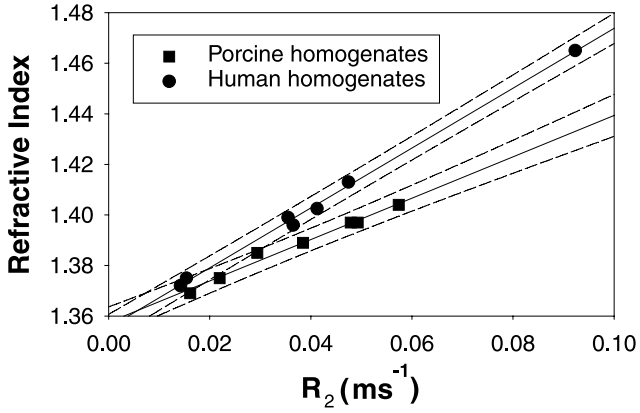

Fig. 2. Refractive index of human and porcine lens homogenates as a function of transverse relaxation rate (R_2) (at 34.5 °C). The solid lines represent the linear best fit, and the dashed lines are the prediction limits (± standard error of the estimate). For the human homogenates: $n = 1.355(\pm 0.002) + 1.18(\pm 0.04)R_2$ (m s^{-1}) ($R^2 = 0.994$, $p < 0.0001$). For the porcine homogenates: $n = 1.358(\pm 0.002) + 0.82(\pm 0.05)R_2$ (m s^{-1}) ($R^2 = 0.98$, $p < 0.0001$).

This implies a direct correlation between the optical and magnetic resonance properties of the human lens. Similar results were found for the porcine lens homogenates, albeit with a different slope (0.819 m s^{-1} compared with 1.184 m s^{-1}). For both human and porcine lenses, results for homogenates derived primarily from cortical or nuclear material were found, within experimental error, to fall on the same line. Differences and/or distributions in refractive indices between different regions of the lens should thus be measurable non-invasively using MRI.

Using the methods described above, we measured R_2 maps of 18 different human lenses of various ages ranging from 14 to 82 years. Representative examples of two human lens R_2 maps of different ages (29 and 82 years) are shown in Fig. 3a and c. Qualitatively it can be seen from these two maps that there are significant dif-

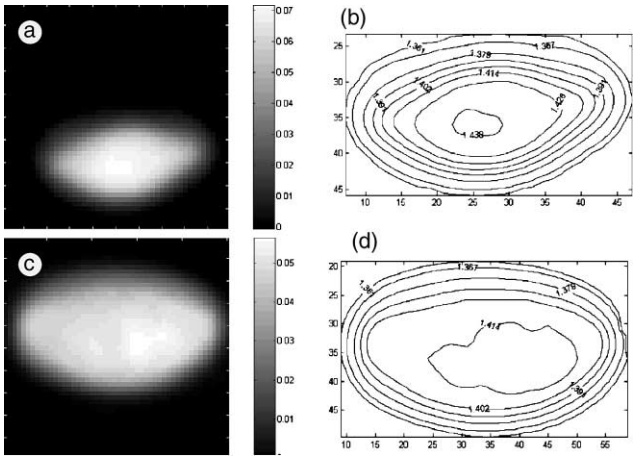

Fig. 3. Transverse relaxation rate images ($m\,s^{-1}$) of a 29-year old human lens (a), with corresponding isoindical contour map (b), compared with that of an 82-year old human lens (c) and corresponding isoindical contour map (d). The FoV in (a) and (c) is 10×10 mm with a 'pixel' size of 0.219 mm, and slice thickness of 1 mm. The scales of the corresponding contour maps are 'numbers of pixels'.

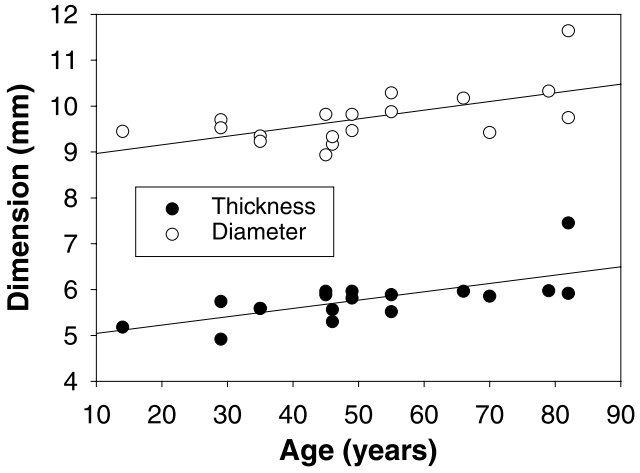

Fig. 4. The distance from anterior to posterior pole (i.e. thickness) and radial diameter of human lenses in vitro (measured from the isoindical contour maps of Fig. 4). For the lens thickness: $t = 4.9(\pm 0.3) + 0.181(\pm 0.005)\text{Age(years)}$ ($R^2 = 0.46$, $p = 0.0019$). For then lens diameter: $b = 8.8(\pm 0.4) + 0.189(\pm 0.007)\text{Age(years)}$ ($R^2 = 0.36$, $p = 0.009$).

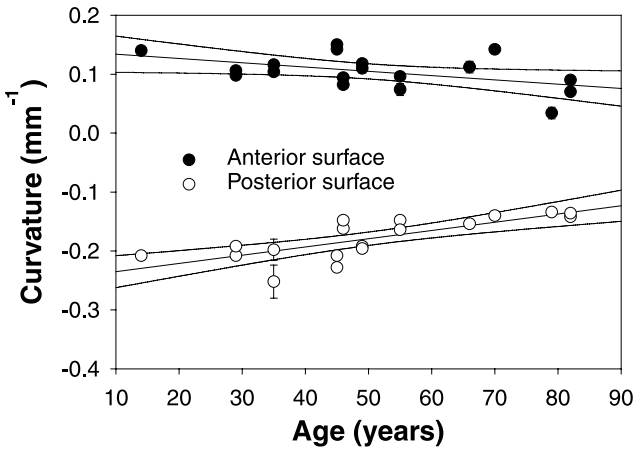

Fig. 5. The anterior (●) and posterior (○) curvatures (C_a and C_p respectively) of human lenses in vitro as a function of lens age. The solid lines represent the least squares best fits and the 95% confidence intervals. The curvatures were calculated by fitting the outer contours of the corresponding contour maps to Eq. (14). For the anterior surface: $C_a = 0.14(\pm 0.02) - 0.0007(\pm 0.0003)\text{Age}$ ($R^2 = 0.23$, $p = 0.045$). For the posterior surface: $C_p = -0.25(\pm 0.02) + 0.0014(\pm 0.0003)\text{Age}$ ($R^2 = 0.58$, $p = 0.0002$).

ferences between them. Firstly, as expected, the older lens is substantially larger than the younger one owing to the continual growth of the human lens throughout life. Secondly, R_2 is more homogeneous over the lens nucleus in the older lens. Thirdly, the magnitude of R_2 in the nucleus of the older lens is lower than that of the lens nucleus in the younger lens. Using Eq. (12) the R_2 maps were converted to contour maps of refractive index (Fig. 3b and d). The lens diameter and thickness were determined by measuring the diameter and thickness of the outer surface contour. The growth of the lens with age was quantified by plotting the lens thickness and diameter as a function of lens age (Fig. 4). The linear regressions in Fig. 4 show that the excised human lens grows linearly in thickness (0.018 ± 0.005 mm/year, $p = 0.002$) and diameter (0.019 ± 0.006 mm/year, $p = 0.009$). The lens surface curvatures in the paraxial region were also calculated by fitting the anterior and posterior sections of the outer contour to an elliptical equation:

$$\frac{z^2}{A^2} + \frac{y^2}{B^2} = 1 \tag{13}$$

and using the fact that the surface curvature in the paraxial region is equal to A/B^2. These values are plotted as a function of age in Fig. 5 for both anterior and posterior surfaces. It can be seen in Fig. 5 that there is a significant ($p = 0.002$) decrease in the magnitude of the posterior lens curvature with age while the anterior curvature shows only a slightly significant ($p = 0.045$) decrease in curvature with age.

From the contour maps of Fig. 3 it appears that the inner isoindical contours do not precisely follow the shape of the lens surface contours and therefore the refractive index distribution, as a function of normalised lens radius, may not be isotropic as assumed in some refractive index models of the human lens. To quantify this observation the profiles of refractive index were plotted as a function of normalised lens radius along the equatorial axis and the anterior and posterior sections of the optical axis for each individual lens. Each profile was then fitted to a sixth order polynomial in the normalised lens radius (Eq. (9)). These profiles and fits are shown for the 82 and 29 year old lenses in Figs. 6 (equatorial

profiles) and 7 (axial profiles), which are typical of the old and younger lenses, respectively.

There is a substantial age difference between the refractive indices corresponding to the centres of the lenses (Figs. 6 and 7) and between the shape of the profiles along the equatorial (Fig. 6) and optical (Fig. 7) axes. The profiles in the equatorial plane also differ from those for the optical axis and there are differences between the anterior and posterior segments of the optical axis in the same lens.

The lens central refractive index and surface refractive index were obtained by non-linear fitting of the profiles to Eq. (9), and plotted as a function of lens age

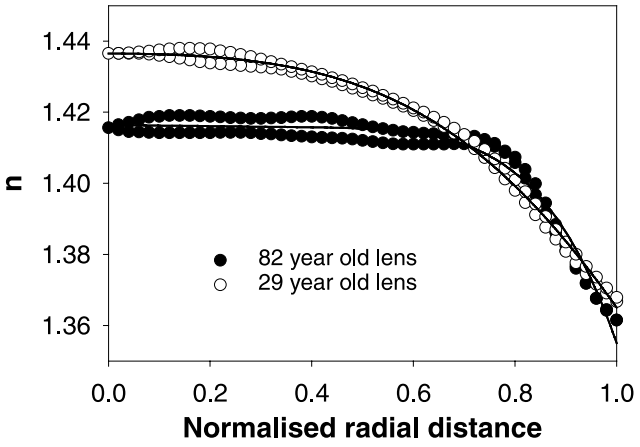

Fig. 6. Examples of refractive index profiles from the centre of the lens nucleus to the lens surface at the equator (in the equatorial plane) obtained from representative old (82 years) and young (29 years) lenses. The solid lines are fits to Eq. (9). The p values for the coefficients are less than 0.001 and r^2 values are greater than 0.98.

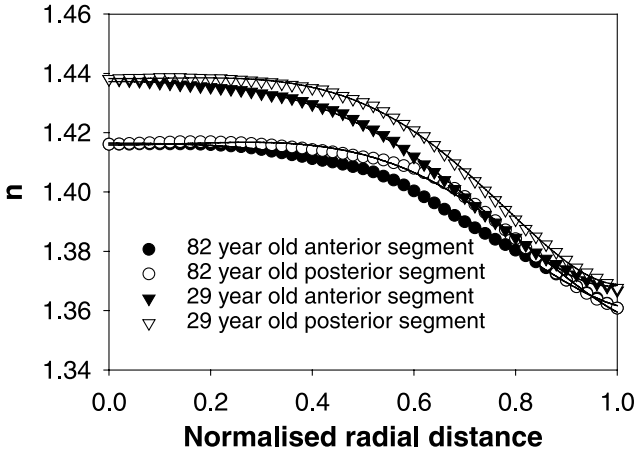

Fig. 7. Examples of refractive index profiles along the optical axis from the centre of the lens nucleus to the lens surface at the anterior pole (filled symbols) and posterior pole (open symbols) obtained from representative old (82 years) and young (29 years) lenses. The solid lines are fits to Eq. (9). The p values for the coefficients are less than 0.001 and r^2 values are greater than 0.98.

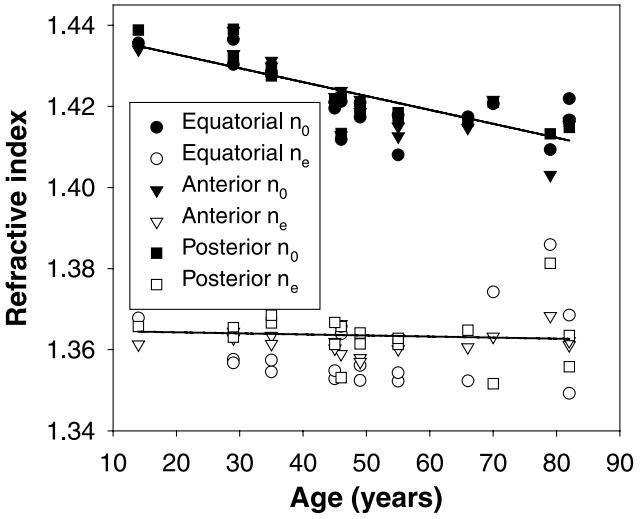

Fig. 8. The least squares regression of lens nuclear (n_0) and surface (n_e) refractive index with age. The parameters n_0 and n_e ($n_0 + n_1 + n_2 + n_3$) were calculated from non-linear least squares fits of the profiles, (see Figs. 6 and 7), to Eq. (9). For the lens surface: $n_e = 1.365\ (\pm 0.005) - 0.00003(\pm 0.00008)$Age ($R^2 = 0.006$, $p = 0.75$). For the lens nucleus: $n_0 = 1.440(\pm 0.003) - 0.00034(\pm 0.00006)$Age ($R^2 = 0.68$, $p < 0.0001$).

(Fig. 8). From the linear regression results in this figure it can be seen that there is a significant decline ($p < 0.001$) in the lens central refractive index with age, while the lens surface refractive index remains constant ($p > 0.05$). Non-linear least squares fitting of the experimental refractive index distributions to Eq. (9) also enabled the shape of the profiles to be quantified in terms of the coefficients n_1, n_2 and n_3. The shapes of the profiles were different along the different axes and were also significantly ($p < 0.001$) dependent on age (Fig. 9). Therefore to estimate F_{GRIN}, Eq. (10) had to be expanded to:

$$F_{\mathrm{GRIN}} \approx -2\left[\left(n_{1,1} + \frac{2}{3}n_{1,2} + \frac{3}{5}n_{1,3}\right)\frac{a_1}{b^2} + \left(n_{2,1} + \frac{2}{3}n_{2,2} + \frac{3}{5}n_{2,3}\right)\frac{a_2}{b^2}\right] \quad (14)$$

where a_1 and a_2 are the anterior and posterior thicknesses respectively, b is the lens sem-diameter, the $n_{1,i}$ coefficients are the results of fitting the anterior profile (Fig. 7) to Eq. (9) and $n_{2,i}$ coefficients are the results of fitting the posterior profile (Fig. 7) to the same equation. F_{GRIN} was estimated for each of the 18 lenses and plotted as a function of age (Fig. 10a). Linear least squares analysis of the plot shows that there is a significant ($p = 0.0006$) decline in F_{GRIN} with age. The paraxial lens power was then estimated for each lens by combining the contributions of F_1, F_2 and F_{GRIN} using Eq. (7). Since the actual distances d_1 and d_2 (the distances from the anterior and posterior poles to the principal

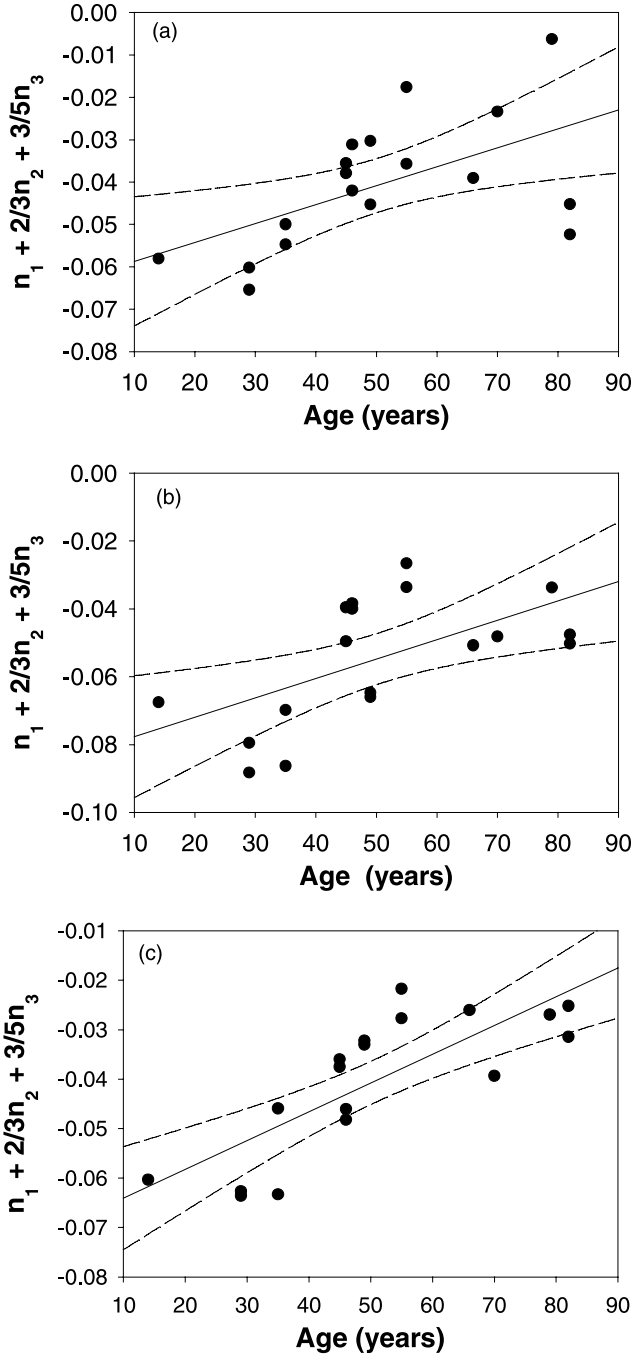

Fig. 9. Least squares regression of the GRIN shape contribution ($n_1 + (2/3)n_2 + (3/5)n_3$) to F_{GRIN} with lens age. The solid lines represent the least squares best fit and the dashed lines the 95% confidence intervals. The parameters n_1, n_2, and n_3 were calculated by non-linear least squares fitting the profiles from Figs. 6 and 7 to Eq. (9). Data for plot (a) were calculated from the profiles along the equatorial axes (Fig. 6), those for plot (b) from the profiles along the anterior optical axes and plot (c) from the profiles along the posterior optical axes. For the equatorial GRIN: $n_1 + (2/3)n_2 + (3/5)n_3 = -0.063(\pm 0.009) + 0.0004(\pm 0.0002)$Age ($R^2 = 0.311$, $p = 0.02$). For the anterior GRIN: $n_1 + (2/3)n_2 + (3/5)n_3 = -0.083(\pm 0.010) + 0.0006(\pm 0.0002)$Age ($R^2 = 0.35$, $p = 0.01$). For the posterior GRIN: $n_1 + (2/3)n_2 + (3/5)n_3 = -0.070(\pm 0.006) + 0.0006(\pm 0.0001)$Age ($R^2 = 0.62$, $p < 0.0001$).

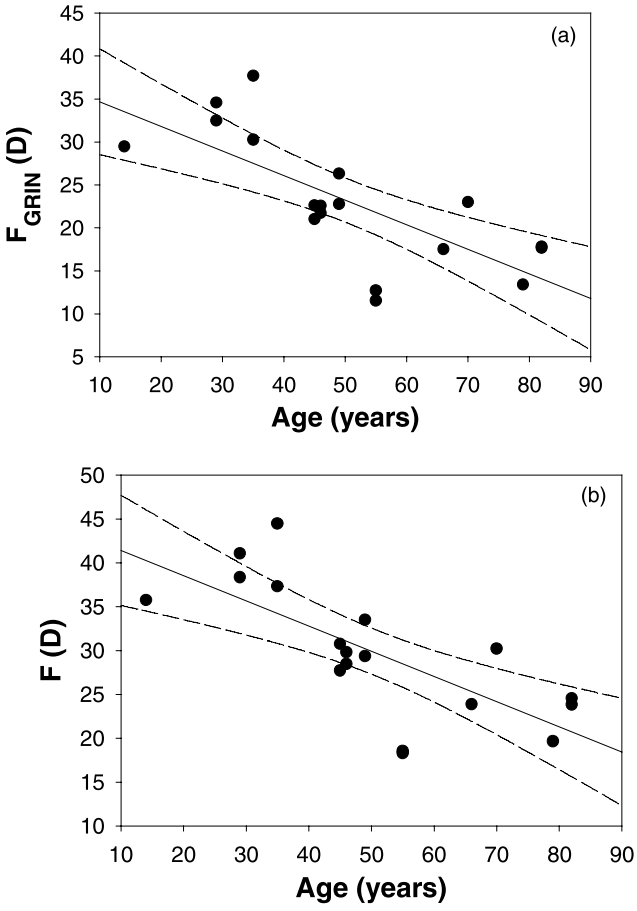

Fig. 10. Least squares regression of the GRIN contribution to lens power (a) and the estimated total lens power (b) as a function of age. The solid lines represent the least squares best fit and the dashed lines the 95% confidence intervals. For the GRIN contribution to lens power: $F_{GRIN} = 37(\pm 4) - 0.286(\pm 0.067)$Age ($R^2 = 0.53$, $p = 0.0006$). For the estimated total lens power: $F = 44(\pm 4) - 0.287(\pm 0.068)$Age ($R^2 = 0.53$, $p = 0.0007$).

planes of the GRIN, respectively) are not precisely known, a_1 and a_2 were used as estimates of these values respectively. Smith et al. (1991) have shown that if all terms in Eq. (7) containing d_1 or d_2 are ignored then the systematic error is not greater than 0.1 D. Therefore it is anticipated that the systematic error in our calculations caused by using a_1 and a_2 will be less than 0.1 D. This is significantly less than the error of the estimated lens power (±5.4 D) derived from the 95% confidence intervals of the linear regression in Fig. 10b. Least squares analysis (Fig. 10b) of these data predicts that the paraxial power of excised human eye lenses decreases significantly ($p = 0.0007$) with age at a rate of ~0.3 D/year. This correlates with the known decrease in accommodative amplitude of ~12 D between the ages of ~10 and 50 years (Glasser & Campbell, 1998; Koretz, Kaufman, Neider, & Goeckner, 1989).

5. Discussion

As indicated previously, it is known that the unaccommodated lens exhibits increased curvature with age while at the same time maintaining emmetropia (or even exhibiting a slight hypermetropic shift), an apparent paradox that has previously been attributed to changes in refractive index distribution (Cook & Koretz, 1995; Pierscionek, 1993; Koretz & Cook, 2001). However confirmation of this interpretation has been limited by the paucity of experimental results for the refractive index distribution in the sagittal plane of the human lens (either in vitro or in vivo). Because of this, attempts to understand lenticular mechanisms of presbyopia and explain the 'lens paradox' have relied on theoretical modelling of the refractive index distribution through the human lens and of possible changes to it with age (Cook & Koretz, 1995; Garner & Smith, 1997; Hemenger et al., 1995; Smith et al., 1992; Smith & Pierscionek, 1998).

Central to the modelling of the human lens is a model for the gradient index (GRIN) distribution. There are currently three commonly used models for the GRIN distribution (Cook & Koretz, 1995). The simplest of these involves replacing the GRIN lens by a lens with a single 'equivalent refractive index' (n_{eq}). In the original Gullstrand–Emsley eye (Emsley, 1952) the equivalent refractive index was assumed to be 1.42, however recently Dubbelman and Van der Heijde (2001a,b) proposed that it should be age dependent, ranging from 1.44 to 1.41. The second model (Smith et al., 1991) is based on experimental results obtained from ray tracing through the equatorial plane (Pierscionek & Chan, 1989). This model suggests that the refractive index distribution is either of the form given by Eq. (9) or alternatively can be characterised in terms of a three parameter power function of the normalised lens radius:

$$n = n_0 + \alpha r^{\rho} \tag{15}$$

where α and ρ are constants and r is the normalised lens radius.

In this model the central and surface refractive indices are kept constant. A change in the shape of the profile, corresponding to a change in either ρ, (Eq. (15)) or n_1, n_2 and n_3, (Eq. (9)), significantly affects the lens power and aberrations (Smith & Pierscionek, 1998; Smith et al., 1991). A third model (Koretz & Cook, 2001) based upon Raman microspectroscopy of local protein concentrations (Siebinga, Vrensen, De Mul, & Greve, 1991) assumes a linear increase in refractive index from the lens surface to a constant value in the nucleus:

$$n(r) = n_0 + \kappa r \tag{16}$$

where κ is a constant.

The first model is obviously a gross over-simplification since the human eye lens is known to be a GRIN lens. It also does not explain the detailed nature of the observed age-dependent decrease in lens power, other than by linking it to a corresponding decrease in the equivalent refractive index. The second and third models are based upon assumptions concerning the form of the GRIN that to date have not been adequately tested. The second model is based upon the assumption of constant lens nuclear and surface refractive indices, combined with a GRIN function based on measurements for the equatorial plane rather than the sagittal plane, and concentric isoindical contours. Results of such modelling show that changes in the shape of the GRIN can plausibly decrease the equivalent refractive index and lens power. The third model is based upon Raman spectroscopic measurements of lens water and protein content that are relatively invasive to the lens. The experimental methods (Siebinga et al., 1991) rely on slicing and fixing the lens in a special solution. Such treatment of the lens has an unknown effect on the local water content. However the data were used by Cook and Koretz (1995) as the basis for inferring lens protein concentrations, which led to the assumption of a linear variation in refractive index through the lens cortex and a constant value in the nucleus. This constant nuclear refractive index as calculated from such modelling was found to decrease (4.3×10^{-4} years^{-1}) with age.

In this study refractive index distributions in the sagittal plane of human lenses have been measured using a magnetic resonance technique. The assumptions on which this method is based are that the refractive index of the lens can be expressed in terms of the empirical linear relationship of Eq. (12), and that this can be inferred from data for human lens homogenates of the form shown in Fig. 2. Although the homogenisation process used for the calibration of the technique disrupts the membrane structure of the lens it does not place the lens proteins under any chemical stress that may change their effect on refractive index. Nor should this process significantly affect the water proton NMR transverse relaxation rates.

As can be seen in Fig. 2 there is a similar relationship for porcine lens homogenates as applies for the human lens, but the gradient of the correlation is significantly different. Such a difference presumably reflects a species difference in the structure and/or biochemistry of the lens proteins. Although the refractive index is governed by the soluble protein concentration the effect of these proteins on transverse relaxation rate is expected to be quite sensitive to protein structure and interactions with the water phase, as well as proton exchange rates. It could be argued that the linear correlations of Fig. 2 may be dependent on the age of the lenses used to make the lens homogenates. Restricted availability of young human lenses (<50 years) meant that the homogenates were all made from lenses in the age range 50–68 years. However we used homogenates made from mixtures of

cortical and nuclear lens tissue as well as homogenates made from solely nuclear or cortical tissue. Due to the growth of the lens these should be representative of relatively old and younger crystallins respectively. All of these homogenates fall on the same linear correlation for both species.

5.1. Implications for lens GRIN models

From the results of Figs. 3, 6 and 7 it is clear that refractive index distribution in the sagittal plane changes significantly with age. By non-linear least squares fitting of Eq. (9) to the experimental profiles in Figs. 6 and 7 it can be seen that the shape of the refractive index profile used by Smith and Pierscionek (1998) and Smith et al. (1991) gives a reasonably good fit to the data. The data also fitted Eq. (15) equally well, but the coefficients in Eq. (9) can readily be used to estimate the GRIN contribution to the lens power using Eq. (10). However it is worth noting that there are some significant departures of the experimental results from the model of Smith et al. (1991) (model 2). Firstly, the isoindical contours are not concentric; hence the shapes of the profiles along the optical (Fig. 7) and equatorial (Fig. 6) axes are significantly different. Secondly, the central refractive index decreases significantly with age (Fig. 8) contributing to the change in coefficients n_1, n_2 and n_3 with age (Fig. 9). Such a decline in refractive index suggests a decline in the nuclear protein concentration (Eq. (1)). Since the lens cells lack the ability to break down proteins and/or remove them from the lens nucleus it is necessary to discuss whether such a finding is plausible and if so how it might occur. Firstly a decline in protein content with increased age has previously been observed in the human lens (Siebinga et al., 1991). The decline in nuclear refractive index also coincides with numerous changes in the lens crystallins including the formation of insoluble aggregates (cf. Hoenders & Bloemendal, 1983). Such a loss of soluble crystallin concentration will directly reduce the refractive index as predicted by Eq. (1).

5.2. Implications for lens equivalent refractive index and lens paradox

The unaccommodated lens increases in curvature with age (Brown, 1974; Dubbelman & Van der Heijde, 2001a). Therefore, provided other optical parameters of the eye remained constant, the eye would be expected to increase in power, resulting in a myopic shift in refractive error. However the refractive error of the eye in general actually shifts in the hypermetropic direction (Saunders, 1981, 1986; Slataper, 1950). This apparent contradiction is known as the 'lens paradox'. To explain the lens paradox it has been suggested that changes to the refractive index or refractive index distribution may compensate for the increase in lens curvature or alternatively that the change in lens curvature may be an attempt by the eye to compensate for changes in refractive index distribution of the lens (Brown, Koretz, & Bron, 1999; Cook & Koretz, 1995). Estimates of equivalent refractive index based on the first model outlined above (Dubbelman & Van der Heijde, 2001a,b) and of nuclear refractive index based on the third model (Cook & Koretz, 1995) have since supported this hypothesis by showing an age-related decrease in both of these parameters. The experimental results of this study (Figs. 6 and 7) provide the first empirical measurements of refractive index distribution that support these explanations of the lens paradox, without the need to assume a particular model for the refractive index distribution in the lens.

The refractive index distributions measured in vitro here are most probably for lenses in their most accommodated state, which itself is expected to be a function of lens age, since older lenses have limited ability to accommodate (see below). However the parameters n_1, n_2 and n_3, can be considered to a first approximation to be independent of lens absolute thickness and radius, and hence independent of accommodative state (Garner & Smith, 1997; Smith & Pierscionek, 1998). If this is the case then the changes in the GRIN distributions observed in this study, that imply an age dependent decrease in F_{GRIN}, should also apply to the unaccommodated lens. It is interesting to note that the rate of decrease in nuclear refractive index ($3.4 \pm 0.6 \times 10^{-4}$ years^{-1}) derived from our data (Fig. 8) is similar to the rate of decrease in equivalent refractive index of $3.9 \pm 0.8 \times 10^{-4}$ years^{-1} previously reported by Dubbelman and Van der Heijde (2001a,b) and of central refractive index (4.3×10^{-4} years^{-1}) reported by Cook and Koretz (1995).

5.3. Implications for presbyopia

Presbyopia is the loss of clear, comfortable near vision due to a decrease in accommodative amplitude of the eye with age. The removal of the lens from the eye as performed in this study removes the external forces of the ciliary body on the lens. Due to the elastic properties of the lens capsule, under these conditions the lens is expected to adopt its most rounded shape, although the extent to which it is able to deform in this way is known to be a function of age. Therefore the lenses used in this study would be expected to be in their most accommodated state. However in the older lenses this is unlikely to be significantly different to their unaccommodated state since their accommodative ability is expected to be negligible.

Recently Glasser and Campbell (1998, 1999) made numerous biometric measurements, (including surface curvatures, lens thickness and diameter, focal length and power), on excised human lenses and found that there

was an age-related decrease in both the power of the accommodated lens and lens curvature. Further, they implied that only changes in lens curvature are needed to explain this age-dependent loss in power of lenses in their most accommodated state since there was a significant linear correlation between lens power calculated from lens curvatures, (assuming a constant equivalent refractive index), and lens power measured from ray tracing experiments (Glasser & Campbell, 1999). However the results of the present study show that an age-related decrease in nuclear refractive index (Fig. 8) and change in GRIN shape occur simultaneously with a decrease in accommodated lens curvature. The decrease (-0.286 ± 0.067 D/year) in F_{GRIN} with age estimated from the regression in Fig. 10a, is not significantly different from the estimated decrease (-0.287 ± 0.068 D/year) in total lens power (Fig. 10b).

These results suggest that, although there is a small decrease in excised lens curvature with age, the effect of this on the accommodated lens power is negligible compared to the effect of the age-related change in refractive index distribution. Such changes to the refractive index distribution have previously been implicated in the cause of presbyopia (Pierscionek, 1993) and supported by lens modelling (Smith & Pierscionek, 1998; Smith et al., 1991), however until now, experimental results did not exist to verify them. The decrease in F_{GRIN} caused by the changes in refractive index distribution with age implies that a greater change in curvature (and accommodative effort) would be required for the aging lens to achieve the same accommodative range as a young lens. Given the increasing size and reduced deformability (Fisher, 1988) of the aging lens, the accommodative amplitude of the lens decreases.

6. Conclusions

Using an empirically determined relationship between lens refractive index and NMR transverse relaxation rate we have shown that NMR micro-imaging can be used to measure the refractive index distribution in the sagittal plane of human lenses. Analysis of refractive index distributions in 18 different human lenses of different ages revealed that the refractive index distribution changes significantly with age, with the main change being a decrease in nuclear refractive index. Age-dependent changes in refractive index distribution have previously been invoked to explain the 'lens paradox' and may contribute to the decrease in maximum accommodative power and accommodative amplitude of the lens that is associated with presbyopia. One possibility is that this may occur due to a decrease in soluble lens crystallins in the nucleus. Although no age-related decrease in total lens crystallins has been observed, an increase in water insoluble lens crystallins with age has been reported previously (Hoenders & Bloemendal, 1983).

Acknowledgements

The authors wish to thank the Queensland and NSW eye banks for supply of human eye lenses. They also acknowledge support for this project from the Australian Research Council. One of us (BAM) also wishes to thank Queensland University of Technology for a postgraduate research scholarship.

References

Atchison, D. A., & Smith, G. (1995). Continuous gradient index and shell models of the human lens. *Vision Research, 35*(18), 2529–2538.

Barer, K., & Joseph, S. (1954). Refractometry of living cells. *Quarterly Journal Microscopy in Science, 95*, 399–423.

Brown, N. (1974). The change in lens curvature with age. *Experimental Eye Research, 19*(2), 175–183.

Brown, N. P., Koretz, J. F., & Bron, A. J. (1999). The development and maintenance of emmetropia. *Eye, 13*(1), 83–92.

Callaghan, P. T. (1991). *Principles of nuclear magnetic resonance microscopy*. Oxford: Oxford University Press.

Carr, H. Y., & Purcell, E. M. (1954). Effects of diffusion on free precession in nuclear magnetic resonance experiments. *Physical Review, 94*, 630–638.

Cook, C. A., & Koretz, J. F. (1995). Modelling the optical properties of the aging crystalline lens from computer processed Scheimpflug images in relation to the lens paradox. In: Vision Science and its applications. OSA Technical Digest Series (pp. 138–141). Washington, DC: Optical Society of America.

Dubbelman, M., & Van der Heijde, G. L. (2001a). The shape of the aging human lens: curvature, equivalent refractive index and the lens paradox. *Vision Research, 41*(14), 1867–1877.

Dubbelman, M., & Van der Heijde, G. L. (2001b). The thickness of the aging human lens obtained from corrected Scheimpflug images. *Optometry and Vision Science, 78*(6), 411–416.

Emsley, H. H. (1952). *Visual optics* (Vol. 1) (5th ed.). London: Hatton Press.

Fisher, R. F. (1988). The mechanics of accommodation in relation to presbyopia. *Eye, 2*(6), 646–649.

Garner, L. F., & Smith, G. (1997). Changes in equivalent and gradient refractive index of the crystalline lens with accommodation. *Optometry and Vision Science, 74*(2), 114–119.

Glasser, A., & Campbell, M. C. (1998). Presbyopia and the optical changes in the human crystalline lens with age. *Vision Research, 38*, 209–229.

Glasser, A., & Campbell, M. C. (1999). Biometric, optical and physical changes in the isolated human crystalline lens with age in relation to presbyopia. *Vision Research, 39*, 1991–2015.

Gullstrand, A. (1909). Appendix II: Procedure of the rays in the eye. Imagery—laws of the first order. *Helmholtz's Handbuch der Physiologischen Optik* (Vol. 1) (3rd ed.) (English translation edited by J. P. Southall, Optical Society of America, 1924).

Hemenger, R. P., Garner, L. F., & Ooi, C. S. (1995). Change with age of the refractive index gradient of the human ocular lens. *Investigative Ophthalmology and Vision Science, 36*(3), 703–707.

Hills, B. P., Takacs, S. F., & Belton, P. F. (1989). The effects of proteins on the proton NMR transverse relaxation times of water. I. Native bovine serum albumin. *Molecular Physics, 67*(4), 903–918.

Hoenders, H. J., & Bloemendal, H. (1983). Lens proteins and aging. *Journal of Gerontology, 38*(3), 278–286.

Koretz, J. F., & Cook, C. A. (2001). Aging of the optics of the human eye: lens refraction models and principal plane locations. *Optometry and Vision Science, 78*(6), 396–404.

Koretz, J. F., & Handelman, G. H. (1986). The lens paradox and image formation accommodating human eyes. *The lens: transparency and cataract, topics in aging research in Europe* (Vol. 6) (pp. 57–64).

Koretz, J. F., Kaufman, P. L., Neider, M. W., & Goeckner, P. A. (1989). Accommodation and presbyopia in the human eye—aging of the anterior segment. *Vision Research, 29*(12), 1685–1692.

Meiboom, S., & Gill, D. (1958). Modified spin-echo method for measuring nuclear relaxation times. *Reviews in Scientific Instruments, 29*(8), 688–691.

Moffat, B. A. (2001). *Nuclear magnetic resonance micro-imaging of the human eye lens.* PhD Thesis, Queensland University of Technology.

Nakao, S., Fujimoto, S., Nagata, R., & Koiti, I. (1968). Model of refractive-index distribution in the rabbit crystalline lens. *Journal of the Optical Society of America, 58*(8), 1125–1130.

Nakao, S., & Ono, T. (1969). Refractive index distribution in the primate crystalline lens and its schematic eye. *Nippon Ganka Kiyo, 20*(5), 533–536.

Pelc, N. J. (1993). Spin preparation and manipulation techniques. In M. J. Bronskill, & P. Sprawls (Eds.), *The Physics of MRI: 1992 AAPM summer school proceedings*. NY: Woodbury.

Pierscionek, B. K. (1993). What we know and understand about presbyopia. *Clinical and Experimental Optometry, 76*(3), 83–90.

Pierscionek, B. K. (1997). Refractive index contours in the human lens. *Experimental Eye Research, 64*(6), 887–893.

Pierscionek, B. K., & Chan, D. Y. (1989). Refractive index gradient of human lenses. *Optometry and Vision Science, 66*(12), 822–829.

Pierscionek, B. K., Chan, D. Y., Ennis, J. P., Smith, G., & Augusteyn, R. C. (1988). Nondestructive method of constructing three-dimensional gradient index models for crystalline lenses: I. Theory and experiment. *American Journal of Optometry and Physiological Optics, 65*(6), 481–491.

Pierscionek, B. K., Smith, G., & Augusteyn, R. C. (1987). The refractive increments of bovine α-, β-, and γ-crystallins. *Vision Research, 27*(9), 1539–1541.

Saunders, H. (1981). Age-dependence of human refractive errors. *Ophthalmic and Physiological Optics, 1*(3), 159–174.

Saunders, H. (1986). A longitudinal study of the age-dependence of human ocular refraction 1. Age-dependent changes in the equivalent sphere. *Ophthalmic and Physiological Optics, 6*(1), 39–46.

Siebinga, I., Vrensen, G. F., De Mul, F. F., & Greve, J. (1991). Age-related changes in local water and protein content of human eye lenses measured by Raman microspectroscopy. *Experimental Eye Research, 53*(2), 233–239.

Slataper, F. J. (1950). Age norms of refraction and vision. *Archives of Ophthalmology, 43*, 466–481.

Smith, G., Atchison, D. A., & Pierscionek, B. K. (1992). Modeling the power of the aging human eye. *Journal of the Optical Society of America A, 9*(12), 2111–2117.

Smith, G., & Pierscionek, B. K. (1998). The optical structure of the lens and its contribution to the refractive status of the eye. *Ophthalmic and Physiological Optics, 18*(1), 21–29.

Smith, G., Pierscionek, B. K., & Atchison, D. A. (1991). The optical modelling of the human lens. *Ophthalmic and Physiological Optics, 11*(4), 359–369.